Measurement and calculation of decay heat in ISIS spallation neutron target

D J S Findlay, G P Škoro, G M Allen, D J Haynes, D M Jenkins and D Wilcox

Published version information

Citation: D Findlay et al. "Measurement and calculation of decay heat in ISIS spallation neutron target." Nuclear Instruments and Methods A, vol. 908 (2018): 91-96.

DOI: 10.1016/j.nima.2018.08.007

Measurement and calculation of decay heat in ISIS spallation neutron target

D J S Findlay, G P Škoro, G M Allen, D J Haynes, D M Jenkins and D Wilcox

Rutherford Appleton Laboratory, Chilton, Didcot, OX11 0QX, UK

Abstract

Thermal powers from radioactive decays (‘decay heat’) within a proton-driven neutron-producing tungsten target on the ISIS Spallation Neutron Source have been measured. Very good agreement is found with calculations using the Monte Carlo code MCNPX.

1. Introduction

In highly irradiated targets on high-power particle accelerators it is often necessary to know what the thermal power from radioactive decays (‘decay heat’) within the target is once the particle beam from the accelerator has been switched off. Usually, decay heats are calculated by Monte Carlo computer codes such as MCNPX [1], since decay heats are not always easy to measure. In principle, decay heat may be measured absolutely by calorimetry once a target has been removed from its operational location, but on a working accelerator facility this may not be practical.

In the present publication, two measurements of the decay heat in the tungsten target in the TS-1 target station on the ISIS Spallation Neutron Source are presented and compared with Monte Carlo calculations using MCNPX.

2. The ISIS TS-1 target and decay heat measurements

The ISIS TS-1 target is a twelve-plate tantalum-clad tungsten target, irradiated by a 40-pulses-per-second (pps) 800-MeV ~180-μA proton beam from the ISIS synchrotron, and cooled by ~500 litres/minute of heavy water. During irradiation the thermal power dissipated within the target is ~100 kW, and the target is instrumented with thermocouples measuring the temperature of each plate. A schematic diagram of the target is shown in Fig. 1.

The decay heat measurements were made essentially by switching off both the proton beam and the flow of cooling water after a long irradiation, and recording the time profiles of the thermocouple temperatures. Two such measurements were made, on 30 November 2016 and on 26 March 2018, in both cases at the ends of ~30-day irradiation campaigns. The temperature data are shown in Figs. 2a and 2b. The vertical range spanned by the data in Fig. 2a is greater than the vertical range in Fig. 2b because in Fig. 2a the water flow through the target was switched off 36 seconds after the beam was switched off, whereas in Fig. 2b the water flow and beam were switched off at the same time; consequently in Fig. 2a there was more time than in Fig. 2b for the bulk of the target to cool down before temperature rises due to decay heat in the absence of water flow became evident.

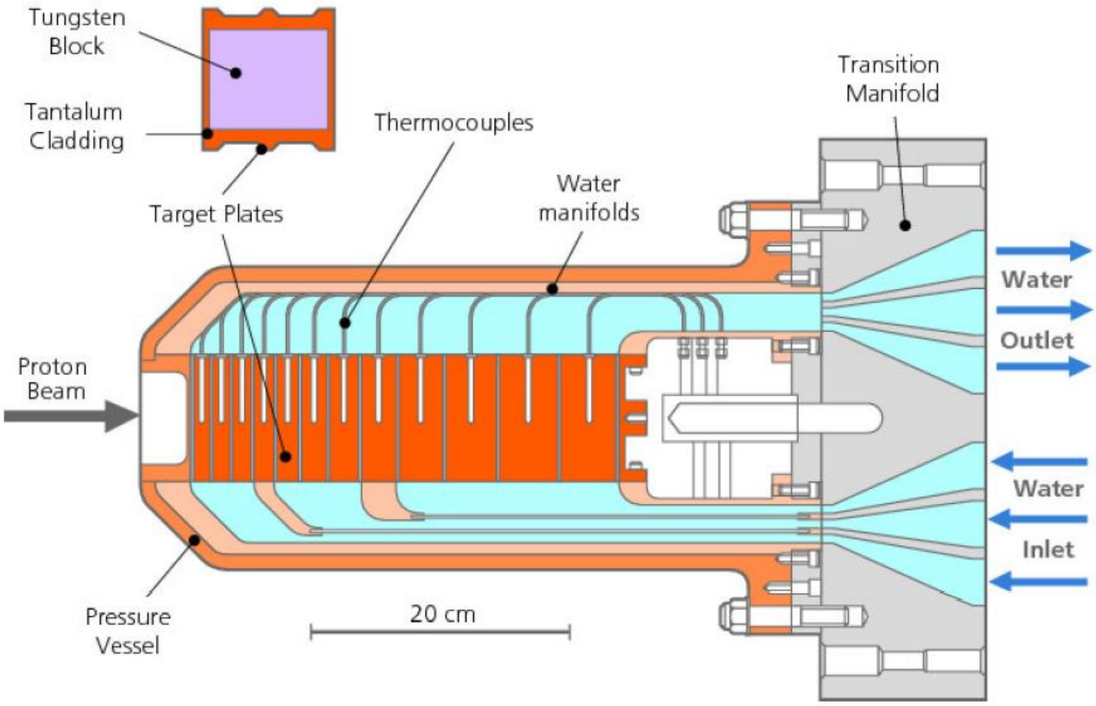

Fig. 1. Schematic diagram of ISIS TS-1 target. Along the direction of the incident beam dimensions are as follows: the thicknesses of tungsten in the target plates are 11.0, 11.0, 12.0, 13.5, 15.0, 18.0, 21.0, 26.0, 34.0, 40.0, 46.0 and 46.0 mm; each plate has 2.0 mm of tantalum cladding on each side; and each plate is separated from its neighbours by 2.0 mm of water. The pressure vessel fits closely over the structures containing and separating the channels through which the cooling water flows.

3. Analysis

The simplest model for each of the target plates is that of an isolated mass m with specific heat c heated internally at a rate $\dot{Q}$ and subject to Newton's Law of Cooling whereby heat flows out of the mass at a rate proportional to the difference between the temperature T of the mass and the (constant) temperature T_s of the surroundings. In such a case the temperature T is described by $T = T_s + (\dot{Q}/\alpha)(1 - \exp(-(\alpha/mc)\ t))$ where α is the constant of proportionality in the law of cooling, whereupon by fitting the expression $T = a + b(1 - \exp(-t/d))$ to the data with a, b and d as three free parameters the internal rate of generation of heat $\dot{Q}$ may be obtained as $\dot{Q} = mc\ b/d$. However, when such a function is fitted to the temperature data shown in Fig. 2 it soon becomes evident that whilst a reasonably good fit may be obtained for the first few tens of seconds after the water flow has been switched off, the function cannot fit the data at longer times; and the reason is, essentially, because there is more than one time constant present in the data.

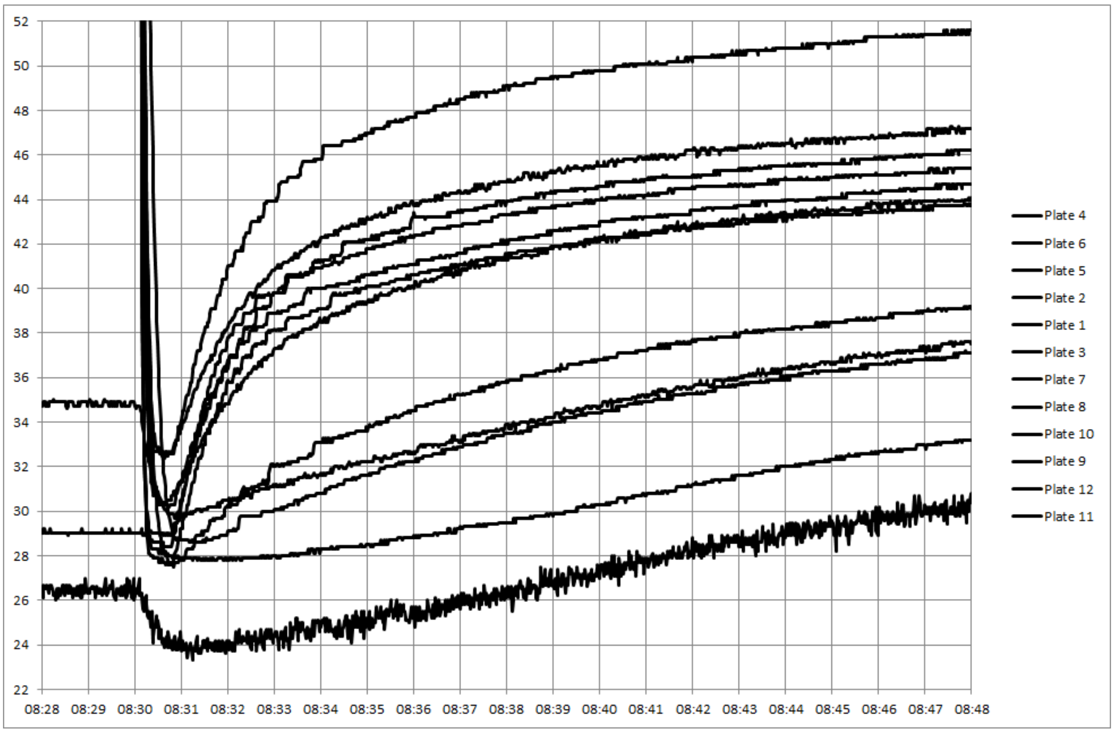

Fig. 2a. 30 November 2016 data. Target plate temperatures (°C) in the TS-1 target as a function of time when the proton beam and water flows were switched off; beam off, 08:30:04; water off, 08:30:40. The order of the curves at 08:35 is the same as the list of plate numbers at the right-hand side.

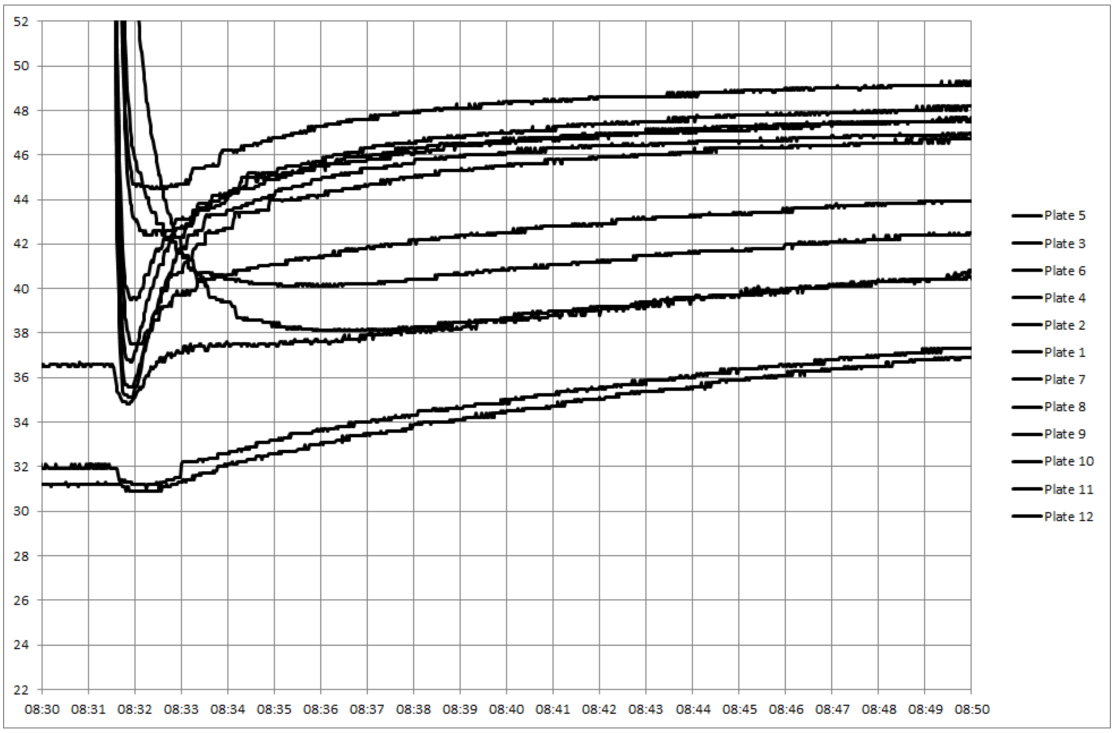

Fig. 2b. 26 March 2018 data. Target plate temperatures (°C) in the TS-1 target as a function of time when the proton beam and water flows were switched off simultaneously; beam and water off at 08:31:28. The order of the curves at 08:35 is the same as the list of plate numbers at the right-hand side. Same horizontal and vertical ranges as Fig. 2a.

A more realistic model is a 'two-mass' model, wherein a target plate at temperature T_1 with mass m_1, specific heat c_1 and internal heat source $\dot{Q}$ is assumed to lose heat at a rate $\alpha(T_1 - T_2)$ to a surrounding assembly at temperature T_2 with mass m_2 and specific heat c_2, and in turn this assembly is assumed to lose heat at a rate $\beta(T_2 - T_s)$ to a thermal sink at temperature T_s, as shown diagrammatically in Fig. 3.

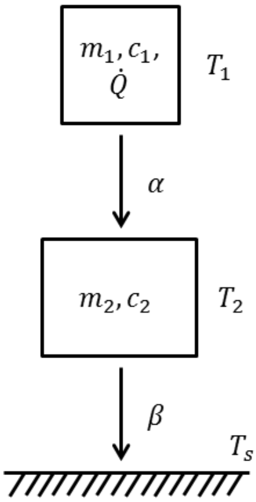

Fig. 3. Diagrammatic representation of two-mass model. Mass m_1 represents a target plate, mass m_2 represents the local surroundings (*e.g.* pressure vessel and associated flanges and manifolds), and the thermal sink represents the more distant surroundings.

For mass m_1, $\dot{Q} = m_1 c_1 dT_1/dt + \alpha(T_1 - T_2)$,
and for mass m_2, $\alpha(T_1 - T_2) = m_2 c_2 dT_2/dt + \beta(T_2 - T_s)$.
By re-arranging the first equation to give an equation for T_2 and then substituting into the second equation, the result is $d^2T_1/dt^2 + a_1\, dT_1/dt + a_2\, T_1 = C$ where $a_1 = (\alpha m_2 c_2 + (\alpha + \beta) m_1 c_1)/(m_1 c_1 m_2 c_2)$, $a_2 = \alpha\beta/(m_1 c_1 m_2 c_2)$, $C = a_2\, T_s + b\, \dot{Q}$, and $b = (\alpha + \beta)/(m_1 c_1 m_2 c_2)$. Using the machinery of the Laplace transform, the subsidiary equation corresponding to the second-order differential equation is, since C is constant,
$(p^2 + a_1 p + a_2)\overline{T}_1 = C/p + pT_1^{(0)} + \dot{T}_1^{(0)} + a_1 T_1^{(0)}$ whereupon by re-arranging as $\overline{T}_1 = (p^2 T_1^{(0)} + p(\dot{T}_1^{(0)} + a_1 T_1^{(0)}) + C)/(p(p^2 + a_1 p + a_2))$ to give the Laplace transform $\overline{T}_1 = \overline{T}_1(p) = \int_0^\infty \exp(-pt) T_1(t) dt$ of the temperature $T_1(t)$, re-writing in terms of partial fractions, completing the square in the quadratic term in the denominator, and then using the shifting theorem and the inverse transforms of the cosh and sinh functions, or by simply looking up a table of inverse transforms (*e.g.* [2]), the solution is

$$\begin{aligned} T_1 &= C/a_2 \\ &+ (T_1^{(0)} - C/a_2 + (\dot{T}_1^{(0)} + (a_1/2)(T_1^{(0)} - C/a_2))/a_{12}) \exp((-(a_1/2) + a_{12})t)/2 \\ &+ (T_1^{(0)} - C/a_2 - (\dot{T}_1^{(0)} + (a_1/2)(T_1^{(0)} - C/a_2))/a_{12}) \exp((-(a_1/2) - a_{12})t)/2 \end{aligned}$$

where $a_{12} = \sqrt{(a_1^2/4) - a_2}$, and $T_1^{(0)}$ and $\dot{T}_1^{(0)}$ are the initial value of T_1 and the initial value of the rate of change of T_1 respectively. Two time constants $1/((a_1/2) - a_{12})$ and $1/((a_1/2) + a_{12})$ are now evident.

However, it is obvious that in reality the target plates are not thermally isolated, and so the simple two-mass model described above was extended to take into account heat flow between plates as shown in Fig. 4.

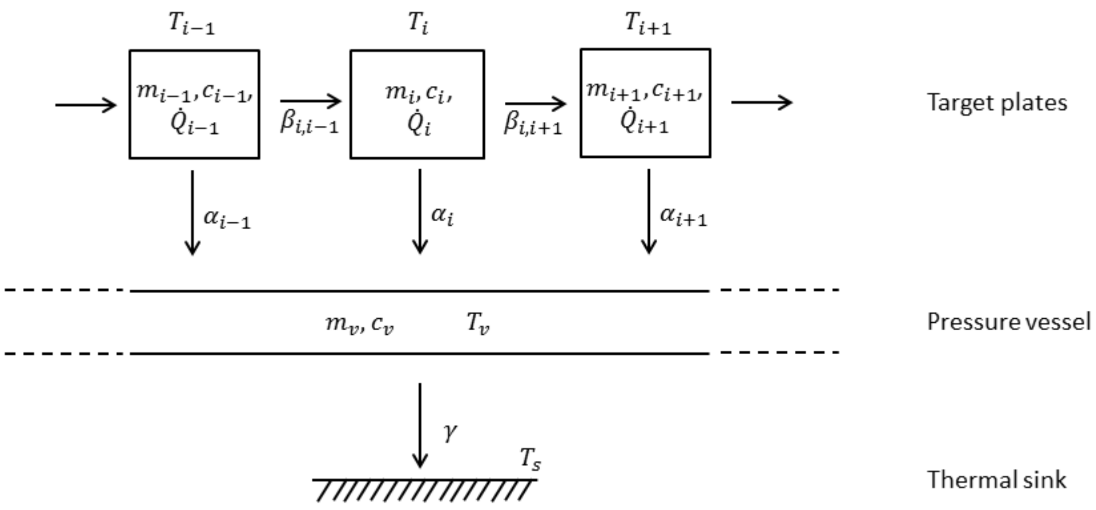

Fig. 4. Extension of the two-mass model to take into account heat transfer between plates.

This extended two-mass model is described by the following set of $n+1$ equations for n plates:

$$\dot{Q}_1 = m_1 c_1 \dot{T}_1 + \beta_{1,2}(T_1 - T_2) + \alpha_1 (T_1 - T_v)$$

$$\beta_{1,2}(T_1 - T_2) + \dot{Q}_2 = m_2 c_2 \dot{T}_2 + \beta_{2,3}(T_2 - T_3) + \alpha_2 (T_2 - T_v)$$

$$\vdots$$

$$\beta_{i-1,i}(T_{i-1} - T_i) + \dot{Q}_i = m_i c_i \dot{T}_i + \beta_{i,i+1}(T_i - T_{i+1}) + \alpha_i (T_i - T_v)$$

$$\vdots$$

$$\beta_{n-2,n-1}(T_{n-2} - T_{n-1}) + \dot{Q}_{n-1} = m_{n-1} c_{n-1} \dot{T}_{n-1} + \beta_{n-1,n}(T_{n-1} - T_n) + \alpha_{n-1} (T_{n-1} - T_v)$$

$$\beta_{n-1,n}(T_{n-1} - T_n) + \dot{Q}_n = m_n c_n \dot{T}_n + \alpha_n (T_n - T_v)$$

$$\sum_{i=1}^{n} \alpha_i (T_i - T_v) = m_v c_v \dot{T}_v + \gamma (T_v - T_0)$$

where the α's represent thermal conductances between the plates and the pressure vessel, the β's represent thermal conductances between pairs of plates, γ represents the thermal conductance between the pressure vessel and the surroundings or thermal sink s, and subscripts i and v refer to plate number and pressure vessel respectively. The solutions of this set of $n+1$ coupled first-order linear differential equations can now be fitted to the plate temperature data as functions of time with the aim of extracting parameters of the fit, especially the decay heats $\dot{Q}_i$.

The set of $n+1$ differential equations was solved by DC04 from the Harwell Subroutine Library (HSL) [3]. But as a check, the equations for a 10-plate test case were also solved by the method of Laplace transforms — taking the transforms of the set of $n+1$ equations above, solving for the resultant temperature transforms $\overline{T}_i$'s and $\overline{T}_v$ using the HSL linear algebra routine ME05, and then numerically evaluating the inverse transform $T_i(t) = \int_{\gamma-i\infty}^{\gamma+i\infty} \exp(pt)\,\overline{T}_i(p)dp\;/\;2\pi i$. A comparison of the two methods of solution for the 10-plate test case is shown in Fig. 5; the agreement is excellent, although a little numerical noise from the inverse Laplace transform is evident.

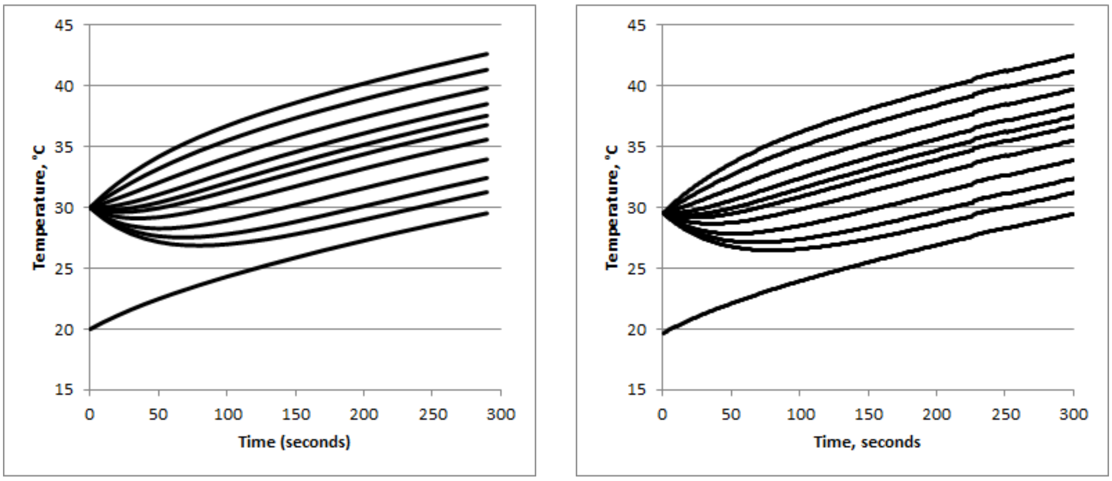

Fig. 5. Time development of plate temperatures by direct solution of coupled differential equations (left-hand side) and by Laplace transforms (right-hand side) (for which γ and '∞' in the equation for the inverse transform were taken as 0.01 and 400 respectively). For both, the order of curves from top to bottom is plate 1, plate 2, plate 3, ... , plate 10, vessel. The parameters assumed were: m's and c's as in Table 1, $\beta = 5$ W °C^{-1} for all plates, $\gamma = 50$ W °C^{-1}, $m_v = 50000$ g, $T_v^{(0)} = 20$°C, $T_s = 20$°C, $T^{(0)} = 30$°C for all plates, $\alpha = 11$, 12, 13, …, 20 W °C^{-1} for plates 1–10, and $\dot{Q} = 162$, 154, 145, 137, 134, 135, 124, 102, 82, and 62 W for plates 1–10 (these $\dot{Q}$'s were taken from preliminary Monte Carlo calculations). Some of the curves initially dip downwards because the internal heat is insufficient to prevent an initial cooling from the starting temperature.

Solutions to the set of $n+1$ coupled first-order linear differential equations solved using DC04 were fitted to the target plate temperature data using the HSL minimisation routine VA04; plate numbers 11 and 12 were excluded because it was reasonably clear from Fig. 2 that decay heat within these two plates is insignificant. It was assumed that all the β's had the same value. Parameters fitted were β, γ, m_v, $T_v^{(0)}$, T_s, $T_1^{(0)}$, $T_2^{(0)}$, … , $T_{10}^{(0)}$, α_1, α_2, … , α_{10}, $\dot{Q}_1$, $\dot{Q}_2$, … , $\dot{Q}_{10}$, a total of 35 parameters, and the function minimised was $\sum_{j,i}(T_{j,i}^{\text{data}} - T_{j,i}^{\text{fit}})^2\,/\delta T_{j,i}^2$ where the sum is taken over temperature datum points j for plate numbers i and $\delta T_{j,i}$ was taken as 0.1°C for all j and i since the temperature data were recorded with a resolution of 0.1°C. The temperature data for all ten plates were fitted simultaneously, although for a given i the only $T^{(0)}$, α and $\dot{Q}$ parameters allowed to vary were $T_i^{(0)}$, α_i and $\dot{Q}_i$. Fixed parameters are given in Table 1. Since the Monte Carlo calculations described in Sect. 4 showed that during the 10 minutes immediately after irradiation ceased the decay heat varied by less than 20%, it was assumed that over the 10-minute fitting interval the decay heat was constant. Results for $\dot{Q}_{\mathrm{tot}} = \sum_i \dot{Q}_i$ after several iterations of VA04 are given in Table 2, and the uncertainties were obtained by repeatedly perturbing all the data points by normally distributed random numbers (from the HSL routine FA05) matched to the uncertainties in the data points and refitting, and then taking the standard deviations of the resultant sets of 'perturbed' values of $\dot{Q}_{\mathrm{tot}}$. The greater uncertainty in $\dot{Q}_{\mathrm{tot}}$ for the 26 Mar. 2018 data is essentially because the (vertical) temperature range spanned by these data is less than it is for the 30 Nov. 2016 data. A typical fit is shown in Fig. 6.

Whilst the number of parameters involved in each of the two fits, 35, is undoubtedly an unusually large number, it should be remembered that the temperature curve for plate i is fitted only by the three parameters $T_i^{(0)}$, α_i and $\dot{Q}_i$ and by a tenth-share in the five parameters β, γ, m_v, $T_v^{(0)}$ and T_s, and so effectively each of the ten temperature curves is fitted by only '3½' parameters, a much more modest number.

	m, g	c, J g^{-1} °C^{-1}
Plate 1	3350	0.1366
Plate 2	3350	0.1366
Plate 3	3570	0.1365
Plate 4	3900	0.1364
Plate 5	4240	0.1363
Plate 6	4900	0.1362
Plate 7	5570	0.1360
Plate 8	6680	0.1359
Plate 9	8450	0.1358
Plate 10	9780	0.1357
Vessel		0.5

Table 1. Values of fixed parameters used in fitting the target plate temperature data. Specific heats c vary very slightly with plate numbers because c_{W} is slightly smaller than c_{Ta} and the tungsten plates become thicker towards the back of the target whereas the thickness of tantalum cladding remains the same. The pressure vessel is stainless steel, hence the different specific heat.

Date	$\varepsilon_{\mathrm{rms}}$, °C	$\dot{Q}_{\mathrm{tot}} = \sum_i \dot{Q}_i$, watts	
		Measured	Calculated
30 Nov. 2016	0.122	1220 ± 90	1130±230
26 Mar. 2018	0.117	1350 ± 240	1320±260

Table 2. Decay heats deduced from the two sets of target plate temperature measurements. $\varepsilon_{\mathrm{rms}}$ is the root-mean-square value of the average deviations between fit and data. The calculated values are from the Monte Carlo computer code MCNPX, and are discussed in Sect. 4. Averaged-over-ten-plates values of the correlation coefficients amongst the fitted $T^{(0)}$, α and $\dot{Q}$ parameters were, for the 30 Nov. 2016 data, 0.48, –0.40 and –0.63, and, for the 26 Mar. 2018 data, 0.94, –0.07 and –0.08 for $\dot{Q}$-α, $\dot{Q}$-$T^{(0)}$ and α-$T^{(0)}$ respectively; the signs of these correlation coefficients are as expected, since, for example, for a given temperature, a higher value of $\dot{Q}_i$ can be partly compensated for by a higher value of α_i. Note that the uncertainties on the calculated decay heats are likely to be almost entirely systematic, and are therefore highly correlated.

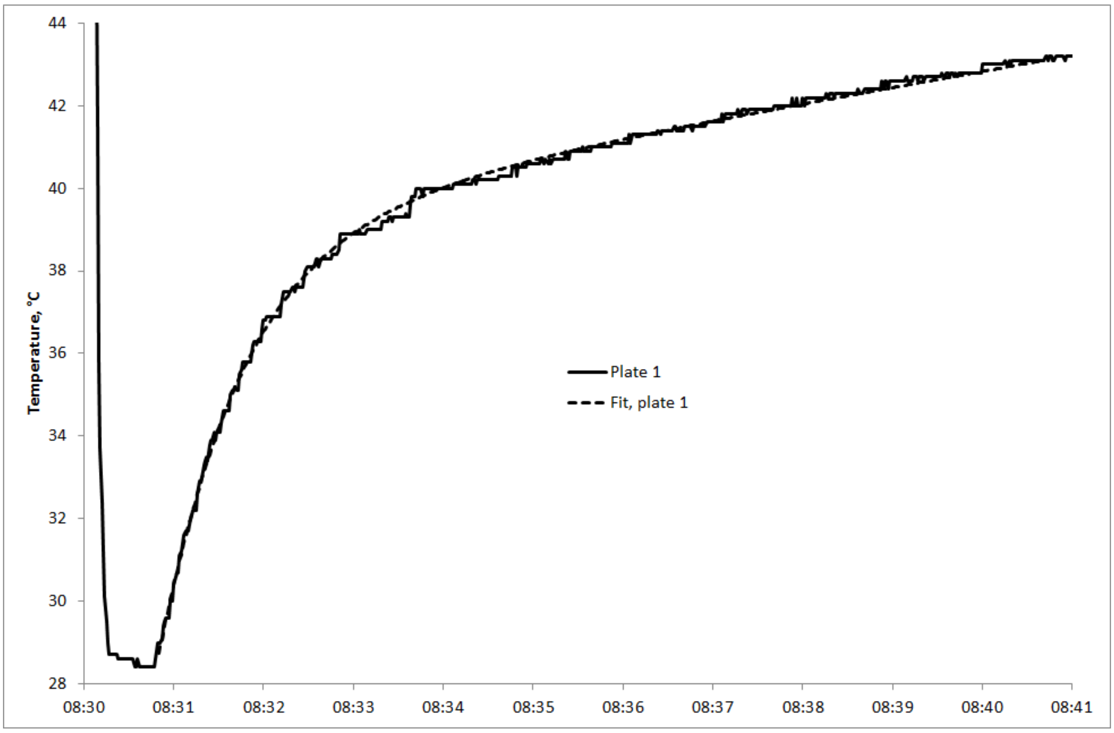

Fig. 6. Fit to data, plate 1, 30 Nov. 2016. The root-mean-square deviation between the fit and the data is 0.12°C.

4. Comparison with Monte Carlo calculations

Calculations were carried out using the MCNPX Monte Carlo code [1] in association with the CINDER'90 transmutation code [4]. A very detailed model of the ISIS TS-1 target-reflector-and-moderators (TRAM) assembly was used (see Section 2 in reference [5]) The model had been built using CombLayer [6], a set of C++ programs which requires the user to effectively write the model geometry into the C++ construction system; this C++ code is then compiled into the final program which, after running, produces the MCNPX input file. Detailed irradiation histories (proton energies[1] and beam currents as functions of time since the target was first irradiated in March 2015) were used for the calculations; the total integrated proton beam currents were 1040 and 1779 milliamp-hours for the 30 Nov. 2016 and 26 Mar. 2018 measurements respectively.

Table 2 also gives the calculated decay heats $\dot{Q} = \sum_k A_k q_k$ (where A_k is the activity of radionuclide k and q_k is its mean decay energy) calculated using MCNPX/CINDER'90 (no further MCNPX calculations were made after the CINDER'90 calculations), and it can be seen that the calculated values agree very well with the measured values. The 20% uncertainties given for the Monte Carlo results are plausible estimates of the uncertainties in the modelling and the nuclear data.

It is obvious that the decay heats do not scale with integrated beam current; this is simply because much of the decay heat is due to ^{182}Ta produced by neutron capture on the tantalum cladding around the tungsten in the target, and the half-life of ^{182}Ta, 115 days, is much less than the overall irradiation times. Table 3 lists the radionuclides that contribute 1% or more to the calculated decay heat immediately after irradiation ceases, and it is clear that ^{182}Ta dominates the list.

Radionuclide	Half-life	% contribution to overall decay heat at $t_{\text{cool}} = 0$	Predominantly produced in
^{182}Ta	115 d	45.80	Ta
^{187}W	23.7 h	4.81	W
^{168}Lu	5.50 m	2.66	W
^{183m}W	5.20 s	2.10	W
^{166}Lu	2.65 m	1.80	W
^{176}Ta	8.08 h	1.77	W
^{166}Tm	7.70 h	1.58	W
^{170}Lu	48.1 h	1.52	W
^{163}Lu	3.97 m	1.12	W
^{171}Hf	12.1 h	1.00	W

Table 3. Radionuclides in the irradiated target ordered by contribution (≥1%) to overall decay heat immediately after irradiation ceases (from the MCNPX/CINDER'90 calculations for 26 Mar. 2018). Also given are the parts of the target (*i.e.* the tungsten 'cores' of the plates, or the tantalum cladding) within which the radionuclides are predominantly produced.

5. Conclusion

Thermal powers from radioactive decays ('decay heat') in an ISIS tungsten target have been measured by fitting a coupled two-mass model to observed temperature dependences of the target plate temperatures when both the proton beam and the cooling water flow are switched off. Decay heats deduced from the measurements agree well with decay heat calculations using the Monte Carlo computer code MCNPX.

[1] During some of the time that the target was being irradiated the synchrotron was running at 700 MeV (rather than its usual 800 MeV) in order to reduce strain on elderly lattice dipoles.

References

[1] MCNPX 2.7.0 — Monte Carlo N-Particle Transport Code System for Multiparticle and High Energy Applications, https://mcnpx.lanl.gov/.

[2] ‘Tables of Integral Transforms’, Vol. 1, McGraw-Hill, 1954, sect. 5.2, page 230, eq. 9, https://authors.library.caltech.edu/43489/1/Volume%201.pdf.

[3] http://www.hsl.rl.ac.uk/.

[4] W L Wilson *et al.*, Proc. SARE4 Workshop, Knoxville, USA, 1998.

[5] G Škoro *et al.*, Physica B: Condensed Matter, 2017, https://doi.org/10.1016/j.physb.2017.12.060.

[6] S Ansell, Proc. ICANS XXI Meeting, Mito, Japan, 2014, JAEA-Conf 2015-002 (2016) p 148–154; https://github.com/SAnsell/CombLayer.